International Journal of Thermal Sciences 49 (2010) 340–348

Contents lists available at ScienceDirect

International Journal of Thermal Sciences

journal homepage: www.elsevier.com/locate/ijts

Experimental study of mixed convection heat transfer in a vertical duct filled with metallic porous structures

G. Venugopal, C. Balaji*, S.P. Venkateshan

Heat Transfer and Thermal Power Laboratory, Department of Mechanical Engineering, Indian Institute of Technology Madras, Chennai 600 036, India

ARTICLE INFO

Article history:
Received 21 October 2008
Received in revised form
29 May 2009
Accepted 17 July 2009
Available online 14 August 2009

Keywords:
Metallic porous structures
Thermo-hydrodynamic performance
Mixed convection
Heat transfer enhancement

ABSTRACT

This paper reports the results of an experimental investigation to examine the potential of a simple and inexpensive porous insert developed specifically for augmenting heat transfer from the heated wall of a vertical duct under forced flow conditions. The porous insert used in the study consists of a stack of metallic perforated plates filled inside the duct. The characteristic features of the porous medium model on the hydrodynamic and heat transfer behavior have been investigated. The porous medium model developed in the present study shows thermo- hydrodynamic performance similar to those seen in metal foams. A correlation has been developed for predicting the Nusselt number from the geometry under consideration. The key novelty in the present work is the development of a new correlation for the Nusselt number that does not require any information from hydrodynamic studies. Over the range of parameters considered, the largest increase in the average Nusselt number of 4.52 times that for clear flow is observed with a porous material of porosity of 0.85.

1. Introduction

Heat transfer in porous media has received great attention for many years due to improved heat transfer performance without a proportionate increase in hydraulic resistance. It is well recognized that a porous structure reduces the boundary layer thickness, increases the surface area in contact with the fluid, intensifies the mixing of the flowing fluid and thereby enhances the convection heat transfer. Flow and heat transfer across channels inserted with porous media have been extensively studies due to their potential applications in thermal management such as compact heat exchangers, electronic cooling, solar collectors, nuclear reactor cooling and packed bed regenerators.

Various types of porous materials have been developed with a specific intention to enhance heat transfer from thermally loaded surfaces. Because of the random structures of porous media, they are different in geometry, physical and thermal properties. Consequently, the flow and heat transfer characteristics in these media also differ significantly. Megerlin et al. [1] experimentally demonstrated the use of mesh and brush inserts to enhance heat transfer in electrically heated circular tube test sections. The authors reported that the use of mesh inserts in tubes increases the heat transfer coefficient about nine times in comparison with empty tubes for the same mass velocities and for the case with brush inserts, the improvement in the heat transfer coefficient was about five times. Renken and Poulikakos [2] investigated, experimentally and numerically, forced convective heat transport in a packed bed of spheres occupying a parallel plate channel whose walls are maintained at constant temperatures. Based on the study, the authors pointed out that the employment of porous media needs to be considered as a viable alternative for heat transfer augmentation in forced convection heat transport in channels. Boomsma and Poulikakos [3] reported the results of experimental studies performed to evaluate the hydraulic characteristics of open cell aluminum foams of various porosities and pore diameters in both compressed and uncompressed form. Their study was mainly concerned with the prediction of two important parameters, permeability and foam coefficient, accurately in order to describe the pressure drop versus flow velocity behavior in porous media. Mixed convection about a horizontal isothermal surface embedded in a water saturated packed bed of spheres was studied experimentally by Renken and Poulikakos [4] and the authors used a scale analysis and concluded that the governing parameter for mixed convection about a horizontal isothermal surface embedded in a porous medium is $Ra_x^{1/3}/Pe_x^{1/3}$. Forced convection in a horizontal channel filled with sintered bronze beads was reported by Hwang and Chao [5]. Their study considered measurement data in both the thermal entrance and thermally fully developed regions, and

* Corresponding author. Tel.: +91 4422574689; fax: +91 4422570509.
E-mail addresses: balaji@iitm.ac.in (C. Balaji), spv@iitm.ac.in (S.P. Venkateshan).

1290-0729/$ – see front matter © 2009 Elsevier Masson SAS. All rights reserved.
doi:10.1016/j.ijthermalsci.2009.07.018

Nomenclature

A	area of the hot wall, m^2
C	form coefficient, m^{-1}
C_p	specific heat of fluid (air), $J\,kg^{-1}\,K^{-1}$
Da	Darcy number $= \frac{K}{D_h^2}$
D_h	hydraulic diameter of the channel, m
f	friction factor
Gr_D	Grashof number based on hydraulic diameter $= \frac{g\beta\Delta T_{avg} D_h^3}{\nu^2}$
Gr_D^*	modified Grashof number $= Gr_D \times Da$
h	average heat transfer coefficient, $W\,m^{-2}\,K^{-1}$
$h(x)$	local heat transfer coefficient along x- direction, $W\,m^{-2}\,K^{-1}$
K	permeability, m^2
k_f	thermal conductivity of fluid, $W\,m^{-1}\,K^{-1}$
k_m	effective thermal conductivity of the porous medium, $W\,m^{-1}\,K^{-1}$
k_s	thermal conductivity of solid (brass), $W\,m^{-1}\,K^{-1}$
L	length of the hot wall or length of the porous medium, m
Nu_D	average convective Nusselt number
Pe	Peclet number
Pe^*	modified Peclet number $= Pe \times Da$
ΔP	pressure drop across the porous medium, $N\,m^{-2}$
Q	heat transfer rate, W
q	heat flux at the wall, $W\,m^{-2}$
Re_D	Reynolds number based on hydraulic diameter
Ri_D	Richardson number based on hydraulic diameter
ΔT_{avg}	average wall temperature with respect to fluid inlet temperature, K
T_{in}	fluid inlet temperature, K
T_w	wall temperature, K
T_f	film temperature $= \frac{T_w + T_{in}}{2}$, K
U	fluid velocity at the inlet, ms^{-1}
W_P	pumping power, W

Greek symbols

α	thermal diffusivity of fluid, $m^2\,s^{-1}$
α_m	effective thermal diffusivity of porous medium $= \frac{k_m}{(\rho Cp)_f}$, $m^2\,s^{-1}$
β	isobaric cubic expansivity of fluid, K^{-1}
μ	dynamic viscosity of fluid, $N\,s\,m^{-2}$
ν	kinematic viscosity of fluid, $m^2\,s^{-1}$
φ	porosity of porous material
ρ	density of fluid, $kg\,m^{-3}$
$x-y$	cartesian coordinates, m

Subscripts

in	inlet
w	wall

correlations for local and fully developed Nusselt numbers were proposed. Calmidi and Mahajan [6] carried out experimental and numerical studies to investigate forced convection in a horizontal channel embedded with high porosity metal foams with due attention given to understand the thermal dispersion and thermal non-equilibrium effects in metal foams. Mohamad [7] presented the results of numerical investigations performed to study the heat transfer enhancement for a flow in a pipe or channel, fully and partially filled with porous medium. Pavel and Mohamad [8] investigated, experimentally, the potential of metallic porous materials, manufactured from aluminum screens, in enhancing forced convective heat transfer from a pipe subjected to a constant and uniform heat flux. The results showed that higher heat transfer rates using porous inserts can be achieved at the expense of a reasonable pressure drop. Later, the authors [9] performed numerical investigations and compared the results of numerical investigations with their experimental results. They pointed out important reasons that negate a direct comparison between the numerical and experimental results. Raju and Narasimhan [10], using a numerical study, presented a novel approach of treating near compact heat exchangers (in-line tube to tube arrangement) as global porous media for estimating the global thermo-hydraulic characteristics. The authors presented correlations for non-dimensional pressure drop and Nusselt number for characterizing the thermo-hydraulic performance of the chosen near compact heat exchanger configurations.

A few studies on heat transfer in porous media filled in vertical channel/annulus have been reported. In a notable work, Pu et al. [11], experimentally, investigated mixed convection in a vertical channel packed with chrome steel spheres, heated asymmetrically. From the experimental observations, the transition regime from natural to forced convection limits was proposed for the geometry considered in their study. Reda [12] studied, experimentally and numerically, mixed convection in a vertical annulus packed with glass spheres and obtained the radial temperature profiles in the bed. In a numerical study, Kwendakwema and Boehm [13] investigated the variation of Grashof, Darcy and Reynolds numbers on the velocities, temperatures and heat transfer between vertical concentric cylinders filled with a porous medium. Choi and Kulacki [14] performed both experimental and numerical investigations on mixed convection through vertical porous annuli locally heated from the inner cylinder. Based on numerical results, the Nusselt numbers were correlated by the parameter groups $Nu/Pe^{1/2}$ and $Ra/Pe^{3/2}$, and the regressed form of Nusselt number was then compared with the experimentally measured Nusselt number.

The above review of literature suggests that most of the previous studies have restricted their attention to metallic porous materials inserted in horizontal channels and scarce are the studies with metallic porous structures inserted in vertical rectangular channels. Furthermore, in earlier studies the porous media that have been employed in the vertical channel/annuli are made of conventional granular beads which have low porosities in the range 0.4–0.6. As far as heat transfer enhancement from the vertical channels is concerned, the employment of porous media other than those made from conventional geometrical shapes remains unexplored. In the present study, a new, simple and inexpensive metallic porous structure is developed with a view to enhance the heat transfer from the heated wall of a vertical rectangular duct under forced flow conditions and the thermo- hydrodynamic performance of the proposed porous structure is investigated experimentally. Finally, the experimentally measured non-dimensional parameters are correlated through linear and nonlinear regression analysis for predicting the heat transfer performance.

2. Experimental set up and procedure

The schematic diagram and a photograph of the experimental setup used to investigate convective heat transfer in a vertical rectangular duct embedded with metallic porous samples are shown in Fig. 1(a) and (b) respectively. The experiment setup composed of a vertical duct, porous media and a plate-heater assembly is built inside the test section of a vertical wind tunnel.

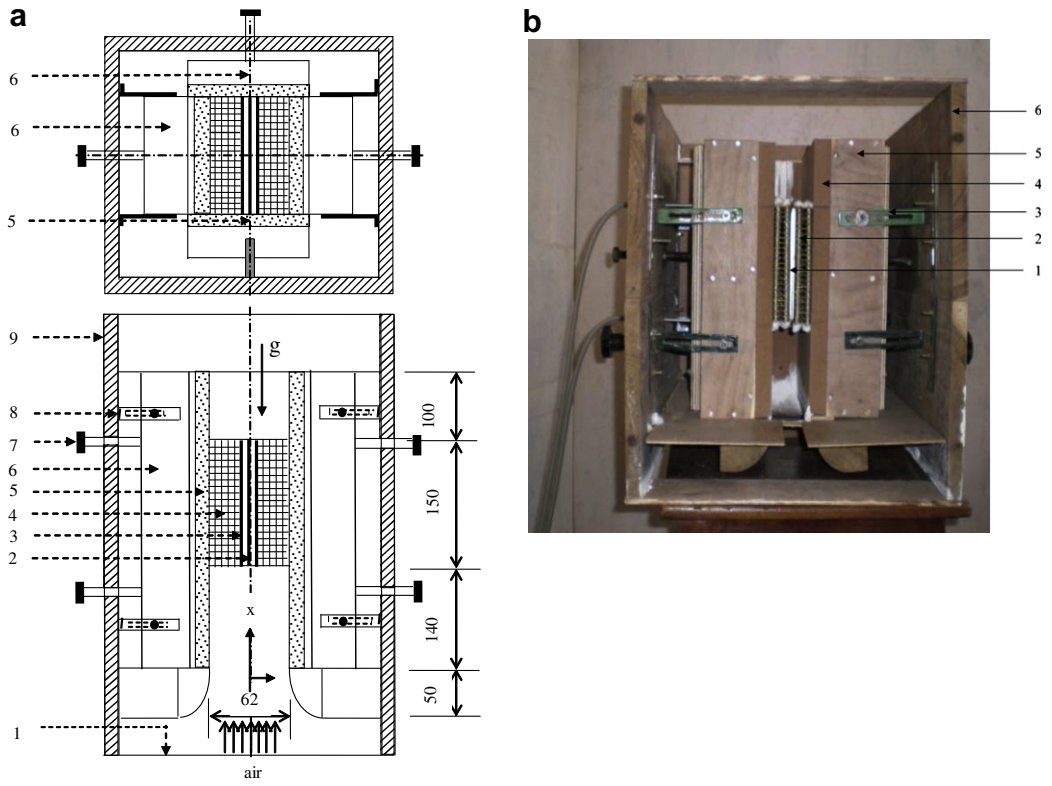

Fig. 1. (a). Schematic of the experimental setup for the study of mixed convection in a vertical duct filled with metallic porous structures. 1. Wire mesh at the inlet. 2. Electric heater. 3. Aluminum plate ($150 \times 250 \times 3$ mm^3). 4. Porous medium. 5. Non-rubberized cork 6. Wooden box. 7. Tightening bolts. 8. L-clamp. 9. Side walls of test section of wind tunnel. (b). Photograph of the experimental setup (One end wall is in removed position). 1. Plate heater assembly. 2. Porous medium. 3. L-clamp. 4. Non-rubberized cork. 5. Wooden box. 6. Side walls of test section of wind tunnel.

The vertical duct is 390 mm × 250 mm × 62 mm and made of 25 mm thick non-rubberized cork supported by wooden boxes made of 12 mm plywood panels. The wooden boxes are fixed to the side walls of the test section of the wind tunnel using 'L' shaped mild steel brackets, two on each side of wooden boxes. The grooves made on the brackets facilitate movement of the walls of the duct along the three coordinate directions and therefore allow the wooden boxes to be fixed at any desired position by means of locking nuts. A nut and screw arrangement, one at the bottom and the other at the top, on the back side of each wooden box permits the walls of the duct to move away from or closer to both vertical center axes of the test section. Such an arrangement helps us keep and align the porous medium and the heater-plate assembly in position and thereby maintain the dimensional accuracy of the test section. Moreover, the non-rubberized cork used for constructing the walls of the duct, due to its cushioning effect, ensures an air tight test section after all locking nuts are tightened properly. A bell mouth is constructed at the entrance to the vertical duct to minimize the entry losses, ensuring uniform flow at the inlet of the test section.

The metallic porous structures used for the experiments are prepared from commercially available 1.5 mm thick perforated brass sheets having stamped holes of 3 mm diameter. Initially, a large number of perforated sheets having slightly larger dimensions than 250 mm × 27 mm are cut from large perforated sheets and a group of such cut-sheets are then given a soft grinding operation to achieve the desired dimensions, i.e. 250 mm × 27 mm × 1.5 mm. After the grinding operation, the edges of each sheet are rubbed with emery paper to remove any burr that would occur during the grinding operation. The perforated sheets are then assembled together by means of washers (1 mm thick) arranged between the perforated sheets and threaded copper rods (3 mmΦ) with fastening nuts positioned at the four corners of the perforated sheets. The perforated plates are assembled in such a way that the holes in the consecutive plates are in staggered fashion so that more residence time and thorough mixing of the fluid is assured. The space between the perforated sheets can be adjusted by adding or removing the washers between them and in this way porous samples of different porosity are obtained. It is worth mentioning that equal numbers of washers are used between successive perforated sheets to obtain a porous sample of desired porosity. Three different porous samples of porosity ($\varphi = 0.85$, 0.89 and 0.92) are prepared for which the number of perforated sheets used are 55, 37 and 23 respectively. In a porous sample, after fabrication, the tip of the copper rods and the fastening nuts extend beyond the sample and they act as protrusions. These protrusions are covered with glass wool to minimize the heat loss to the fluid. Fig. 2 shows the photograph of a porous sample ($\varphi = 0.92$) prepared for the experimental study.

The plate-heater assembly essentially consists of two aluminum plates of dimensions 150 mm × 250 mm × 3 mm with a flat heater sandwiched between them. The flat heater is formed by winding a Nichrome wire over a mica sheet and the heater is electrically insulated from the unexposed side of the aluminum plates by using thin mica foils. The two halves of the heater-plate assembly are joined together by means of fastening screws and nuts. A counter sinking operation given to all holes ensures proper seating of fastening screws and nuts. Ten "K- type" (36AWG) stainless steel sheathed thermocouples, five on each aluminum plate, are used for the measurement of temperatures at several locations of the heated plate. They are fixed to the plates using copper cement that has a high thermal conductivity. All thermocouples are calibrated before fixing them into the grooves machined in the plates and the

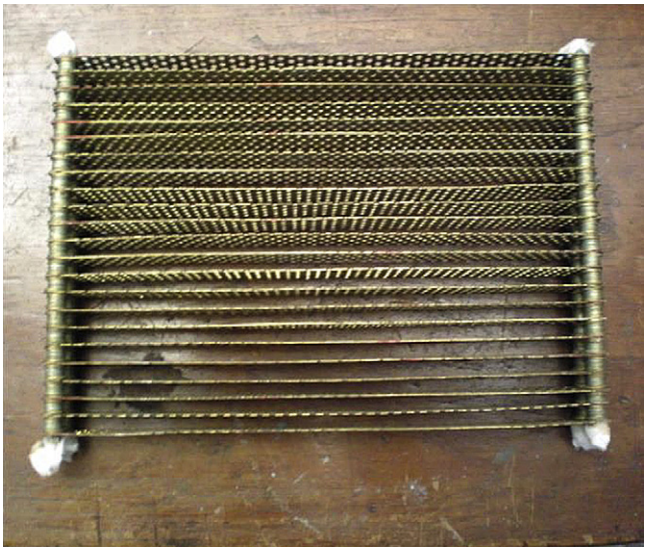

Fig. 2. Photograph of a porous sample ($\varphi = 0.92$).

maximum measurement error is within ±0.2 °C. The thermocouples are connected to a PC based Data acquisition system (Model No.34970A, Agilent Technologies Ltd.) through compensating wires. The power input to the heater is supplied from a regulated DC power source which has a range of 30–600 V and 0–1.5 A. The power input to the heater is calculated by measuring the voltage and current using digital multimeters.

The test section inside the vertical duct is made by fixing two identical porous samples, one on either side of the plate-heater assembly. The resulting physical dimensions of the vertical rectangular duct embedded with porous samples are 150 mm × 250 mm × 27 mm, with one of the vertical walls heated and the other being adiabatic. The velocity and temperature of the air at the inlet of the test section are measured using a thermal anemometer (AIRFLOW™ TA5). Using an arrangement for traversing the anemometer, the velocity measurement is done at ten different locations upstream of the test section and the mean value of the velocities is used for calculating the Reynolds number. The air velocity is varied by varying the speed of the axial flow fan mounted appropriately below the diffuser entry. The pressure drop across the porous sample is measured by a digital differential pressure transducer connected to pressure taps located at the inlet and outlet of the test sample. The test section can be heated to different temperature levels by controlling the input to the heater. The fluid temperature at the outlet of the test section is recorded by three K-type stainless steel sheathed thermocouples located just above the test section. Among the three thermocouples, two are located just above the porous sample placed on one side of the plate-heater assembly and the third thermocouple is located above the porous sample placed on the other side of the plate-heater assembly. It is observed that the maximum temperature variation among the three thermocouples is within ±0.6 °C and this indicates that symmetry prevails about the vertical axis of the test section. A comparison of fluid enthalpy rise with the electric power input shows that the maximum heat loss from the test section is less than 6% for a power input ranging from 8 to 105 W.

Experiments are conducted for all porous samples at different mass flow rates and power inputs to the heater. The procedure followed during an experiment run is as follows. The axial flow fan is switched ON and its speed is adjusted using an electronic control panel to obtain the desired flow velocity at the inlet of the test section. After the flow is stabilized, the velocity and temperature of the air at the inlet of the test section are measured. The test section is then heated by supplying a known amount of electrical power and the heated wall is allowed to reach steady state conditions. Steady state is deemed to be reached when the temperature of the heated wall is observed to vary within ±0.1 °C in ten minutes. During a typical experiment run, the inlet and outlet fluid temperatures, pressure drop across the test section, the local wall temperatures, fluid velocity at the inlet and electrical power input are measured. The experiments were repeated for several power inputs to the heater (corresponding heat flux value ranges from 215 to 2800 W/m^2) and different flow velocities at the inlet of the test section. The thermophysical property values for air are estimated at the film temperature, T_f.

3. Results and discussion

3.1. Hydrodynamic performance

The understanding of the behavior of fluid flow through porous medium is of great importance in several engineering fields. As far as a porous medium is concerned, porosity, permeability and form coefficient are the three hydrodynamic parameters that characterize the behavior of fluid flow through the medium. The volume based porosity (φ) of the samples is determined by evaluating the ratio of the void volume to the total volume of the samples. The void volume is determined by filling distilled water inside the sample. The porosity of the samples is rechecked by determining the volume fraction of solid which is defined as the ratio of dry mass of the porous sample to the mass corresponding to total volume of material measured by its geometry. The dry mass of the sample is measured by an electronic balance having a resolution of 0.01 g. The mass corresponding to total volume of material is calculated from the product of density of the material of the sample and total volume of the sample measured from its geometry. Three porous samples ($\varphi = 0.85$, 0.89 and 0.92) are used for the study and, as mentioned earlier, they are prepared by varying the spacing between consecutive perforated plates.

The permeability and form coefficient of each porous sample are experimentally determined by measuring the pressure drop across the porous sample at different fluid inlet velocities. Fig. 3 represents the variation of measured pressure drop per unit length of porous samples with the fluid velocity at the inlet. A least square fit is performed to determine the variation of measured pressure drop per unit length versus the fluid velocity. The least square fit shows that a second order polynomial curve, as represented by Eq. (1) follows the trend of data points very well.

$$\frac{\Delta P}{L} = AU + BU^2 \tag{1}$$

The results of pressure drop studies show that the flow behavior of the porous samples prepared for the present study deviates from the Darcy law. The physical phenomenon responsible for the quadratic term in Eq. (1) is the drag force imposed on a fluid by any solid surface obstructing the flow path. Incorporating the drag force in Darcy equation, the modified form of Darcy equation known as the Hazen–Dupuit–Darcy equation is given by

$$\frac{\Delta P}{L} = \frac{\mu}{K}U + \rho C U^2 \tag{2}$$

By comparing equations (1) and (2), the values of K and C are calculated as

$$K = \frac{\mu}{A}, \quad C = \frac{B}{\rho} \tag{3}$$

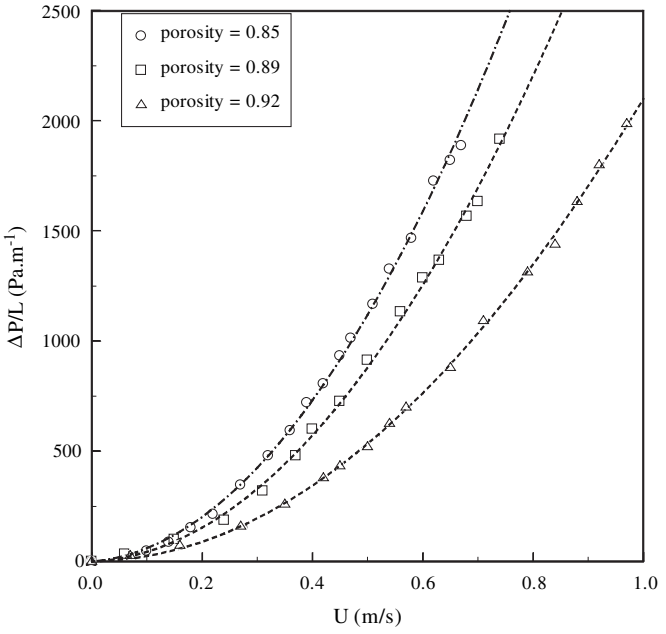

Fig. 3. Variation of pressure drop across the porous medium with the fluid velocity at the inlet.

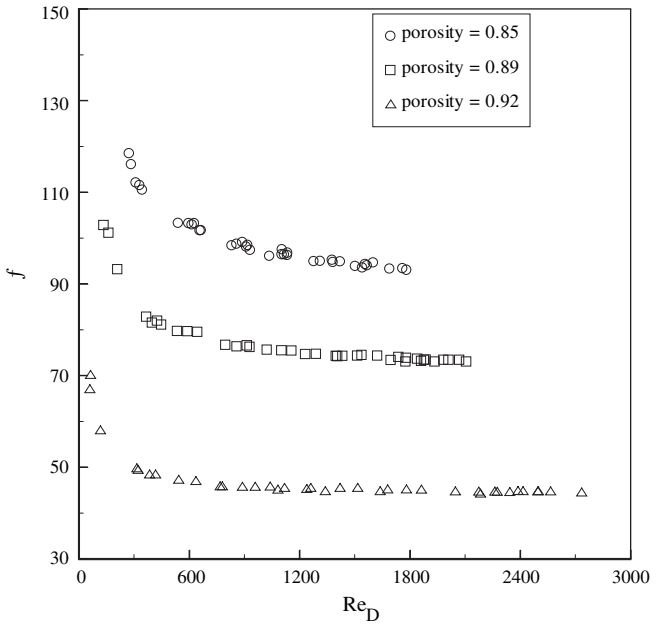

Fig. 4. Friction factor versus the Reynolds number for different porous media.

Table 1 lists the permeability and form coefficient for the porous samples tested. A large value of form coefficient indicates that the pressure drop is governed primarily by the form drag. It is evident from the Fig. 3 that the pressure drop in the porous medium increases with decreasing porosity and increasing flow rate, as expected. As the porosity decreases, the surfaces area to volume ratio increases creating additional flow resistance. This leads to an increase in the pressure drop.

The fanning friction factor, f based on the hydraulic diameter of the channel is calculated as defined by Eq. (4) reported in [15].

$$f = \frac{\Delta P}{4\left(\frac{L}{D_h}\right)\left(\frac{\rho U^2}{2}\right)} \tag{4}$$

Fig. 4 shows the friction factor, calculated from the experimental data, plotted against the channel Reynolds number for different porous media used. The plots illustrate that the friction factor is affected by the porosity of the tested samples, i.e. a low porosity medium offers high flow resistance. As was mentioned earlier, a low porosity porous medium can be prepared by increasing the number of perforated plates. So the friction factor also increases which is intuitively apparent. A comparison of the fanning friction factor calculated from the present experimental work with those reported in [16] for metal foams indicates that the friction factor of the porous samples is of the same order as that of metal foams. A look at the curves in Fig. 4 shows that the friction factor curves level off after a Reynolds number of approximately 1200. A similar trend was reported in [16] for metal foams too. However, it is important to mention that the Reynolds number calculated in [16] is based on the permeability of the metal foams, whereas in the present work the Reynolds number is based on the hydraulic diameter of the channel.

Table 1
Hydrodynamic characteristics of the porous samples used in the experimental study.

Medium	Porosity (φ)	Permeability (K), m^2	Form coefficient (C), m^{-1}	Darcy No.
1	0.85	1.06×10^{-7}	3.575×10^{3}	4.452×10^{-5}
2	0.89	1.83×10^{-7}	2.888×10^{3}	7.684×10^{-5}
3	0.92	5.83×10^{-7}	1.789×10^{3}	2.450×10^{-4}

3.2. Heat transfer performance

The commercially available perforated brass plates, used for the preparation of metallic porous structures, are examined for their metallurgical composition using a Scanning Electron Microscope (Make: FEI-Czech Republic, Model-QUANTA 200). The results of micro analysis show that the metallurgical composition of the tested specimens are Cu K (57.34 wt %), Zn K (31.49 wt %), C K (8.80 wt %) and O K (2.37 wt %). The thermal conductivity for a wide variety of copper based alloys usually ranges from 116 to 123 W/m K [17]. Since the metallurgical composition of the tested specimens is close to a copper based alloy with Cu (60%) and Zn (40%), for the present experimental investigations the thermal conductivity of the solid material of the porous samples, k_s is chosen as 123 W/m K which corresponds to the thermal conductivity of brass with Cu (60%) and Zn (40%) [17]. The effective thermal conductivity of the porous structures is then calculated as the weighted geometric mean of k_f and k_s, defined as [18]

$$k_m = k_f^{\varphi} k_s^{1-\varphi} \tag{5}$$

The various thermal and flow parameters needed to characterize the thermal performance of the porous medium are calculated for various experimental measurement conditions and they are defined according to the following expressions.

The local heat transfer coefficient, $h(x)$ is defined in terms of the temperature difference between the heated wall and the inlet temperature of the fluid when the power dissipation at the wall is known.

$$h(x) = \frac{q_w}{(T_w(x) - T_{in})} \tag{6}$$

Using the measured power dissipation at the wall and the difference between the average wall temperature and the fluid inlet temperature, the average Nusselt number is defined as

$$Nu_D = \frac{q_w D_h}{k_m \Delta T_{avg}} \tag{7}$$

where the average wall temperature with respect to fluid inlet temperature is defined as

$$\Delta T_{avg} = \frac{\sum_{j=1}^{n} T_{wj}}{n} - T_{in} \tag{8}$$

The modified Grashof number is calculated using the following relation:

$$Gr_D^* = Gr_D \times Da = \frac{g\beta \Delta T_{avg} D_h K}{\nu^2} \tag{9}$$

The Peclet number is computed as

$$Pe = \frac{UD_h}{\alpha_m} \tag{10}$$

where α_m denotes the effective thermal diffusivity of the porous medium.

The Reynolds and the Richardson numbers are defined based on the hydraulic diameter of the duct and they are determined, respectively, from the following expressions.

$$\mathrm{Re}_D = \frac{UD_h}{\nu} \tag{11}$$

$$Ri_D = \frac{Gr_D}{\mathrm{Re}_D^2} \tag{12}$$

The Colburn j factor which characterizes the heat transfer performance of a heat exchanging device is given by

$$j = \frac{h}{\rho CpU}\left(\frac{\nu}{\alpha}\right)^{2/3} \tag{13}$$

Fig. 5 presents the distribution of the local heat transfer coefficient along the dimensionless distance of the heated wall for the three values of porosity, tested at the same heat input and Reynolds number. As seen from this figure, the local heat transfer coefficients in all the cases decrease with the increase in the dimensionless distance x/L, since the heat transfer coefficient is based on the temperature difference with respect to the inlet temperature. This trend is expected as the largest temperature gradient between the heated wall and the incoming cold fluid occurs at the inlet of the test section. Consequently, the highest heat transfer rate occurs at the bottom of the channel. As the fluid moves up into the channel, the local fluid temperature increases thereby effectively increasing the local wall temperature and reducing the local heat transfer coefficient along the flow direction. It is also seen that the porous medium with the lowest porosity is more effective in enhancing the rate of heat transfer than the porous medium with high porosities. Fig. 6 shows the results for the average Nusselt number with Reynolds number for three porosities. As the Reynolds number increases, the Nusselt number increases, as expected. It is further seen that the influence of Reynolds number on the heat transfer rate is more predominant in high porosity samples. A high porosity medium offers a comparatively lower resistance for the fluid to penetrate through the porous medium. Therefore, one would expect that the increasing porosity would increase the fluid velocity inside the porous medium. High porosity causes flow redistribution and intensifies the mixing of the flowing fluid stream, leading to increased heat exchange between the fluid stream and the solid matrix of the porous medium. However, for a given heat input and a fixed Reynolds number, the Nusselt number increases with decreasing porosity and this will be discussed later.

A qualitative measure of the potential of the porous materials to enhance the rate of heat transfer from the heated wall of the duct is given by the average wall temperature with respect to the fluid inlet temperature, as defined in Eq. (8), at different Reynolds numbers, monitored for cases with and without porous inserts. Fig. 7 shows the average wall temperature with respect to the fluid inlet temperature at different Reynolds numbers, recorded with and without porous inserts at a given heat input of 104.6 W. A drastic drop in the average temperature of the wall compared to those without porous materials confirms a dramatic increase in

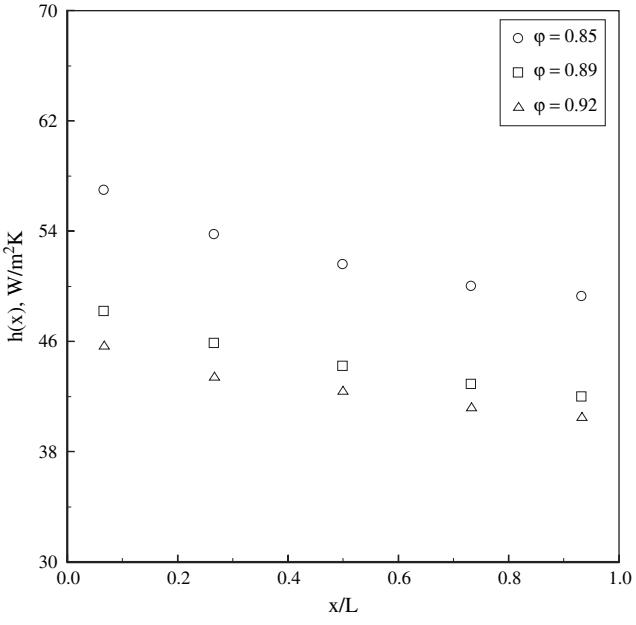

Fig. 5. Distribution of the local heat transfer coefficient along the dimensionless distance of the heated wall.

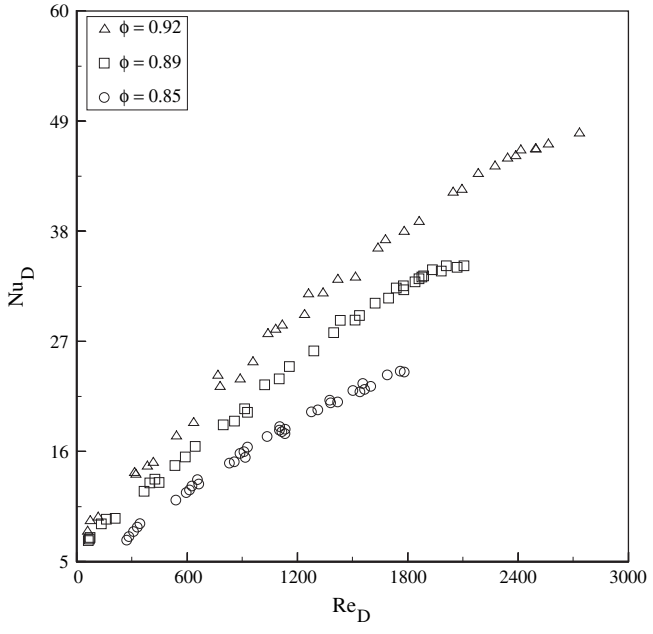

Fig. 6. Average Nusselt number as a function of Reynolds number for different porous media.

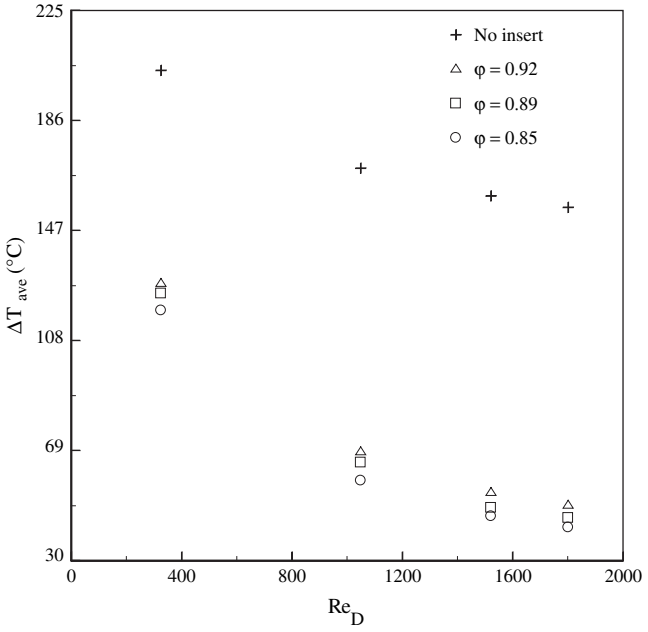

Fig. 7. Measured average wall temperature ΔT_{avg}, with and without porous inserts for different Reynolds numbers.

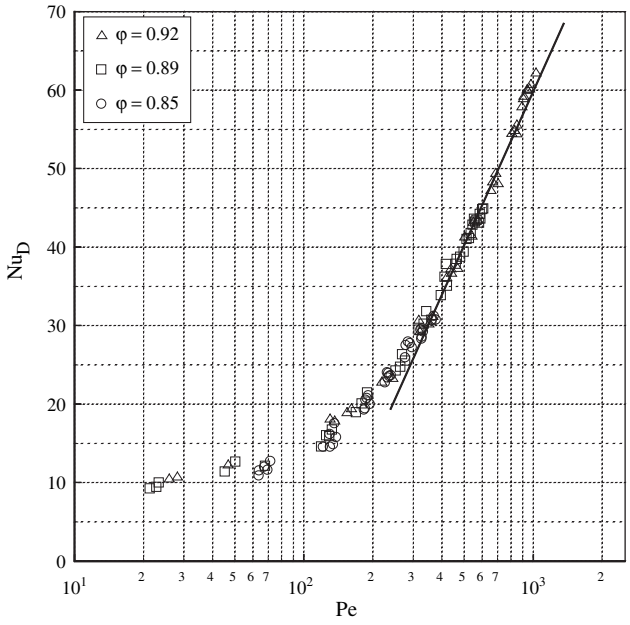

Fig. 8. Average Nusselt number as a function of the Peclet number.

heat transfer in the presence of porous inserts. Moreover, among all the porous samples examined, the average wall temperature is least for the case with low porosity material inserts at a given Reynolds number The large enhancement in heat transfer can be attributed to the fin effect of the perforated plates touching the heated wall and the high degree of turbulence produced by the large number of minute holes of the perforated plates. In general, the possible factors contributing to heat transfer process in a porous material made of perforated plates can be, (1) increased effective surface area; (2) increased conduction heat transfer resulting from contact between the perforated plates and the wall surface; (3) enhanced mixing of fluid stream due to large local flow velocities within the porous insert; and (4) increased turbulence due to jet like flow through the holes of the perforated plates. The first two factors promote heat transfer through fin effect and the last two factors promote heat transfer coefficient through enhanced turbulence [19,20]. The foregoing discussion implies that the fin effect has a profound effect on heat transfer in low porosity porous samples. Furthermore, the high effective thermal conductivity and the large heat capacity of a low porosity porous sample strengthen the fin effect. This means that there is a significant heat exchange between the fluid and solid matrix for the low porosity porous sample due to fin effect, in addition to the heat transfer caused by turbulence. As a result of this, among the present porous inserts, the low porosity porous sample provides the least wall temperature at a given Reynolds number. Finally, in order to represent the heat transfer enhancement quantitatively, the average Nusselt number estimated corresponding to ΔT_{avg} (Fig. 7) recorded for low porosity porous sample at different Reynolds numbers is compared with the average Nusselt number estimated corresponding to ΔT_{avg} recorded for clear flow case. The comparison shows that the increase in the average Nusselt number with porous medium insert is 1.89 and 4.52 times higher than that for the clear flow case, respectively, at Reynolds numbers 352 and 1802. From this analysis, it is clear that even for low flow rates, significant improvement in heat exchange is achieved with the proposed porous structure.

The average Nusselt number on the heated wall as a function of the Peclet number is depicted in Fig. 8. This figure indicates a general increase in average Nusselt number with increasing Peclet number because the average wall temperature with respect to the fluid inlet temperature ΔT_{avg} generally decreases as the Peclet number increases. A close examination of the Fig. 8, however, shows that the dependence of Nusselt number on Peclet is unique for$Pe \geq 300$. Hence, we infer that forced convection is fully dominant for Peclet number greater than approximately 300. A different trend observed in the experimental data for Peclet number less than approximately 300 can be interpreted as due to buoyancy effects on forced convection flow. This suggests that for low Peclet number flows, the buoyancy effects on heat transfer need to be considered jointly with effect of inertia force on heat transfer, especially for the case of heat transfer from vertically oriented surfaces. It must be noted that the modified Grashof number, defined as the product of Grashof number and Darcy number, is chosen as the buoyancy parameter in this study. Since the range of Darcy number studied is very narrow, the criterion based on modified Grashof number for delineating the heat transfer regimes namely natural, mixed, and forced convection dominant has not been considered in this study.

The Colburn j factor plotted against the Reynolds number in Fig. 9 shows a general decrease in Colburn j factor with increasing flow rate. A similar characteristic was reported in [16] for metal foams. A reasonably high value of Colburn j factor reveals that higher heat transfer rate is possible with lower flow rates. Finally, to report the overall heat transfer characteristics of the proposed porous inserts, the experimental data for average Nusselt number is expressed a function of modified Grashof number and Peclet number. A multiple linear regression analysis results in the following correlation for the average Nusselt number.

$$Nu_D = 1.10 Gr^{*0.05} Pe^{0.544} \quad (14)$$

$$\begin{bmatrix} 2.9 \leq Gr^* \leq 180 \\ 21 \leq Pe \leq 1030 \end{bmatrix}$$

Equation (14) is developed using 114 experimental data, has a correlation coefficient of 0.99 and the standard deviation of error is ±0.1. The Peclet number exponent is close to 0.5, normally seen in

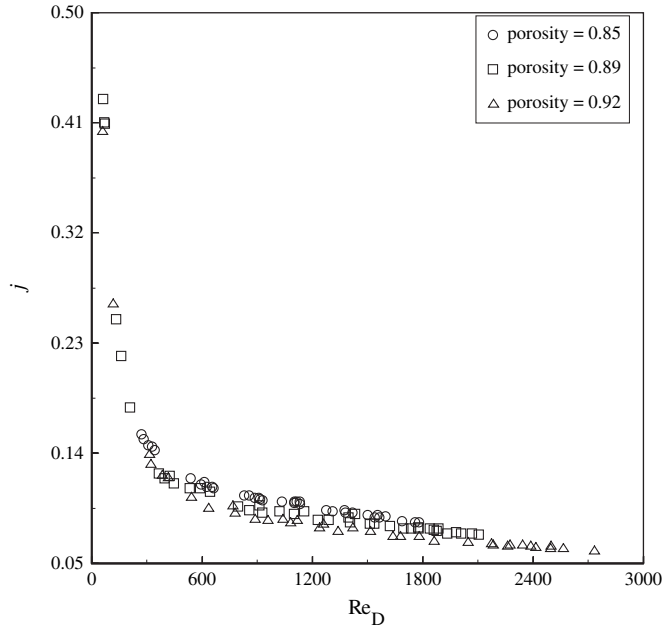

Fig. 9. Colburn *j* factor versus the Reynolds number for different porous media.

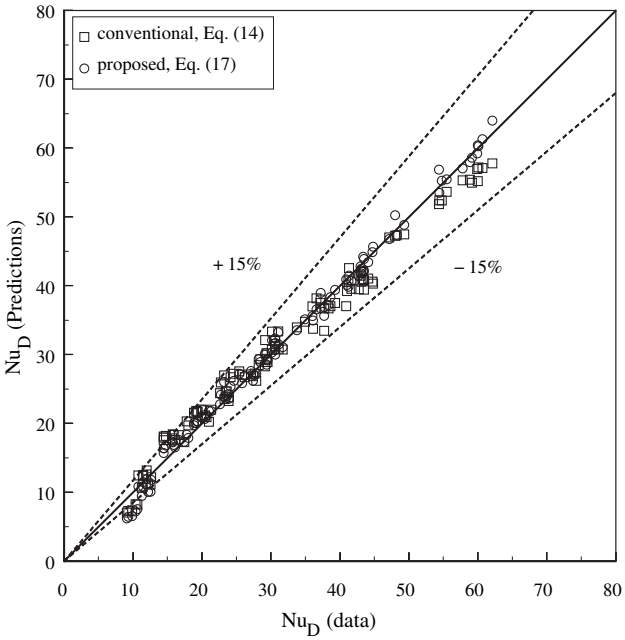

Fig. 10. Parity plot showing the agreement of the Nusselt numbers predicted using the conventional and the proposed approach.

laminar flows. In Eq. (14), representing the heat transfer performance of the porous medium, the Darcy number represents the hydrodynamic parameter controlling the heat transfer performance which needs to be experimentally determined by measuring the pressure drop across the porous medium. However, Darcy number is directly associated with the porosity of the medium. So a Nusselt number correlation which incorporates the porosity instead of Darcy number would be useful for the direct estimation of Nusselt number with out looking for any information from hydrodynamic tests. With this in view, the functional form of the heat transfer correlation is modeled as

$$Nu_D = f(Ri_D, Pe^*) \tag{15}$$

where Pe^* is the modified Peclet number defined as the product of Peclet number and Darcy number. For the given channel dimensions the hydraulic diameter is a constant. So the Darcy number becomes essentially a function of permeability of the porous inserts. For the present study, the dependence of permeability on porosity is expressed through a second order polynomial function. Replacing the Darcy number with the porosity, Eq. (15) can be expressed as

$$Nu_D = a\left(\frac{Ri_D}{1+Ri_D}\right)^b \left(Pe(c\varphi^2 + d\varphi + e)\right)^f \tag{16}$$

where the parameters *a*, *b*, *c*, *d*, *e* and *f* are to be determined. A nonlinear regression analysis is carried out to retrieve the values of the parameters *a*, *b*, *c*, *d*, *e* and *f* and the final form of Eq. (16) turns out to be

$$Nu_D = 1.366\left(\frac{Ri_D}{1+Ri_D}\right)^{-0.034} Pe^{0.563}\left(0.6734\varphi^2 + 0.5391\varphi - 0.3367\right)^{0.563} \tag{17}$$

Equation (17) is also based on 114 data, has a correlation coefficient of ±0.99 and a standard deviation of error of ±1.25. The Nusselt numbers estimated using the correlating equations (14) and (17) are compared in Fig. 10 in the form of a parity plot. The figure indicates that the Nusselt numbers estimated using both correlating equations are in good agreement. This validation study confirms the correctness of the proposed approach for developing a Nusselt number correlation (Eq. (16)), in terms of a directly measurable hydrodynamic parameter of the porous inserts along with the other influencing non-dimensional parameters pertinent to the problem. It is, therefore, inferred that the proposed approach is appropriate for developing a Nusselt number correlation for problems of similar kind. However, it needs to be noted that the Nusselt number correlation as given by Eq. (16) is not a general form of heat transfer correlation applicable to all porous materials.

The heat transfer per unit pumping power as a function of flow Reynolds number is considered to characterize the thermal performance of the porous insert against the flow friction. In Fig. 11,

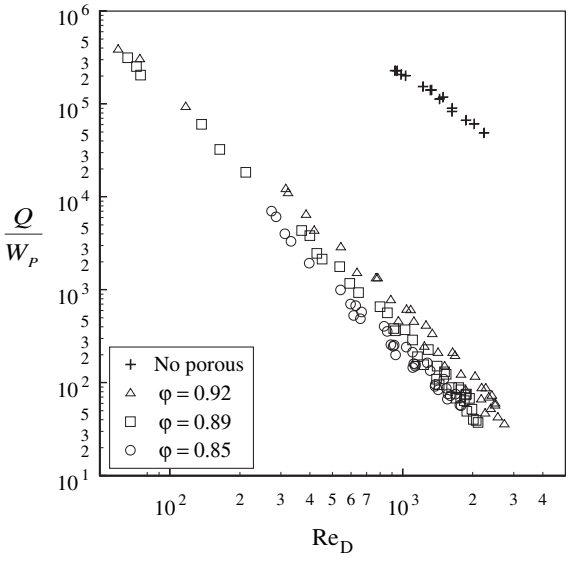

Fig. 11. Heat transfer rate per unit pump power as a function of Reynolds number.

the variation of heat transfer per unit pumping power with respect to flow rate is plotted for all porous inserts and clear flow cases. As pumping power increases with the flow rate, Q/W_P decreases linearly for all cases, as expected. As seen from the figure, for a given ratio of heat transfer to the work input, the low flow rate demand for porous inserts is a clear indication of the usefulness of a porous medium to achieve higher heat transfer coefficient as far as a heat exchange device is concerned. This observed trend is in accordance with variation of '*j*' factor with Reynolds number plotted in Fig. 9. On the other hand, for a given flow rate a comparatively large value of heat transfer rate per unit power input achieved with clear flow case is mainly due to a marginal flow resistance. Even though Q/W_P is high for the no insert case, both Q and W are significantly lower compared to cases with inserts. Hence, in situations where our primary objective is heat dissipation, as is often the case, the additional sacrifice in terms of the increased pumping power can be tolerated. Hence, Fig. 7 that actually shows the tremendous drop in wall temperature with porous inserts suggesting superior thermal performance has to be read in conjunction with Fig. 11 in order that we finally arrive at a good measure of the thermal performance of the system.

4. Uncertainty analysis

The uncertainties in the measured primary physical quantities are obtained from a calibration of the instruments or the uncertainty prescribed by the manufacturer. The propagation of error due to the uncertainties in the measured primary physical quantities into the estimation of Nusselt number is calculated using the procedure described in [21].

The uncertainty, σ_S, in the dependent variable 'S' is given by

$$\sigma_S = \pm\left\{\sum_{i=1}^{n}\left[\left(\frac{\partial S}{\partial x_i}\right)^2 \sigma_{X_i}^2\right]\right\}^{1/2} \tag{18}$$

where '*x*' stands for the independent variable and σ_x is the uncertainty associated with '*x*'.

Following this procedure, the uncertainty in the estimation of heat flux is 2%, hydraulic diameter is 0.19%, effective thermal conductivity is 0.05%, average wall temperature with respect to fluid inlet temperature is 0.64% and the resulting uncertainty in the convective Nusselt number is estimated as 3.65%.

5. Conclusions

A simple inexpensive metallic porous material is developed for heat transfer enhancement application and its thermo-hydrodynamic performance has been investigated experimentally. The pressure drop characteristics of the porous materials are found to follow the Hazen–Dupuit–Darcy model, indicating that the pressure drop is due to combined effect of viscous and form drag. Results indicate that at a given heat input and a fixed Reynolds number, the Nusselt number increases with decreasing porosity. Over the range of parameters considered, the porous insert of smallest porosity ($\phi = 0.85$) gives the best heat transfer performance for which the highest increase in the average Nusselt number is approximately 4.52 times higher than that for clear flow case, accompanied by a moderate pressure drop of 289 Pa(gauge). Finally, a Nusselt number correlation has been proposed that requires no information from the hydrodynamic behavior of the porous medium, except the porosity.

References

[1] F.E. Megerlin, R.W. Murphy, A.E. Bergles, Augmentation of heat transfer in tubes by use of mesh and brush inserts, ASME J. Heat Transfer (1974) 145–151.
[2] K.J. Renken, D. Poulikakos, Experiment and analysis of forced convective heat transport in a packed bed of spheres, Int. J. Heat Mass Transfer 31 (1988) 1399–1408.
[3] K. Boomsma, D. Poulikakos, The effects of compression and pore size variations on the liquid flow characteristics in metal foams, ASME J. Fluids Eng. 124 (2002) 263–272.
[4] K.J. Renken, D. Poulikakos, Mixed convection experiments about a horizontal isothermal surface embedded in a water-saturated packed bed of spheres, Int. J. Heat Mass Transfer 33 (1990) 1370–1373.
[5] G.J. Hwang, C.H. Chao, Heat transfer measurement and analysis for sintered porous channels, ASME J. Heat Transfer 116 (1994) 456–464.
[6] V.V. Calmidi, R.L. Mahajan, Forced convection in high porosity metal foams, ASME J. Heat Transfer 122 (2000) 557–565.
[7] A.A. Mohamad, Heat transfer enhancements in heat exchangers fitted with porous media, Part I: constant wall temperature, Int. J. Thermal Sci. 42 (2003) 385–395.
[8] B.I. Pavel, A.A. Mohamad, Experimental investigation of the potential of metallic porous inserts in enhancing forced convective heat transfer, ASME J. Heat Transfer 126 (2004) 540–545.
[9] B.I. Pavel, A.A. Mohamad, An experimental and numerical study on heat transfer enhancement for gas heat exchangers fitted with porous media, Int. J. Heat Mass Transfer 47 (2004) 4939–4952.
[10] S.K. Raju, A. Narasimhan, Porous medium inter connector effects on the thermo hydraulics of near compact heat exchangers treated as porous media, ASME J. Heat Transfer 129 (2007) 273–281.
[11] W.L. Pu, P. Cheng, T.S. Zhao, An experimental study of mixed convection heat transfer in vertical packed channels, J. Thermophys. Heat Transfer 13 (1999) 517–521.
[12] D.C. Reda, Mixed convection in a liquid saturated porous medium, ASME J. Heat Transfer 110 (1988) 147–154.
[13] N.J. Kwendakwema, R.F. Boehm, Parametric study of mixed convection in a porous medium between vertical concentric cylinders, ASME J. Heat Transfer 113 (1991) 128–133.
[14] C.Y. Choi, F.A. Kulacki, Mixed convection through vertical porous annuli locally heated from the inner cylinder, ASME J. Heat Transfer 114 (1992) 143–151.
[15] W.M. Kays, A.L. London, Compact Heat Exchangers, third ed. McGraw-Hill, New York, 2002.
[16] D. Boomsma, D. Poulikakos, F. Zwick, Metal foams as compact high performance heat exchangers, Mech. Mater. 35 (2003) 1161–1176.
[17] ASM Metals Handbook, Properties and Selection of Non Ferrous Alloys and Special Purpose Materials, 10th ed., vol. 2, ASM International Hand Book Committee, 1990, 265–345.
[18] D.A. Nield, Estimation of the stagnant thermal conductivity of saturated porous media, Int. J. Heat Mass Transfer 34 (1991) 1575–1576.
[19] P.X. Jiang, Z. Wang, Z.P. Ren, B.X. Wang, Experimental research of fluid flow and convection heat transfer in plate channels filled with glass or metallic particles, Exp. Therm. Fluid Sci. 20 (1999) 45–54.
[20] S.C. Tzeng, T.M. Jeng, Y.C. Wang, Experimental study of forced convection in asymmetrically heated sintered porous channels with/without periodic baffles, Int. J. Heat Mass Transfer 49 (2006) 78–88.
[21] S.P. Venkateshan, About Measurement and Errors in Measurement – Mechanical Measurements, first ed. Ane Books India, New Delhi, 2008, pp. 5–25.